THE JOURNAL OF PHYSICAL CHEMISTRY C

Article

pubs.acs.org/JPCC

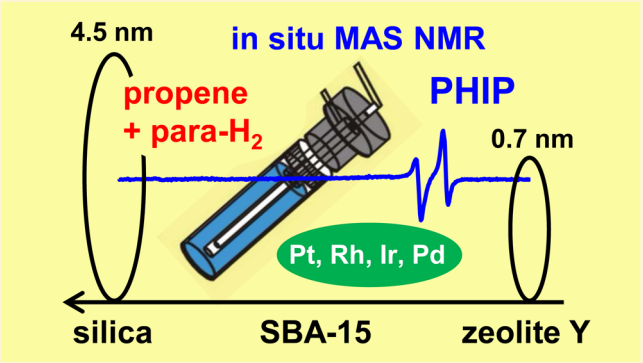
Parahydrogen-Induced Hyperpolarization inside Meso- and Micropores of Pt-, Rh-, Ir-, and Pd-Containing Solid Catalysts

Utz Obenaus, Swen Lang, Robin Himmelmann, and Michael Hunger*

Institute of Chemical Technology, University of Stuttgart, 70550 Stuttgart, Germany

Supporting Information

ABSTRACT: Homologous series of solid catalysts (silica, SBA-15, dealuminated zeolite DeA−Y, zeolite H,Na−Y) with different pore sizes and loaded with different noble metals (Pt, Rh, Ir, Pd) were applied for the gas phase hydrogenation of propene with para-enriched hydrogen (p-H_2) with the aim to produce parahydrogen-induced polarization (PHIP). This hyperpolarization formed by the pairwise incorporation of p-H_2 into propene was studied via in situ ^{1}H MAS NMR spectroscopy under continuous-flow conditions. By evaluating the characteristic ^{1}H NMR antiphase signals of the hyperpolarized reaction products, the experimental parameters and properties of noble-metal-containing porous catalysts were investigated, which affect the formation and relaxation of PHIP. For the catalysts under study, small pore diameters and interactions of the hyperpolarized product molecules with nuclei inside the pores, such as framework aluminum atoms and extra-framework sodium cations, were found to enhance the relaxation of the hyperpolarization formed by the pairwise incorporation of p-H_2 into olefinic reactants. Furthermore, a very high hydrogenation activity of the noble-metal-containing catalyst (Pd/H,Na−Y) decreases the formation of PHIP, possibly caused by a too large number of reactive spillover H species without spin correlation, which hinders the pairwise incorporation of p-H_2 into the olefinic reactants.



1. INTRODUCTION

One of the strategies for enhancing the sensitivity of solid-state NMR spectroscopy for the investigation of heterogeneously catalyzed reaction systems is the coupling of the nuclear spins under study to a reservoir of nuclei with much higher polarization,[1] such as by utilizing parahydrogen-induced polarization (PHIP).[2−4] In the case of a pairwise incorporation of the two H atoms of parahydrogen molecules with a total nuclear spin of $I = 0$ into olefins, the initial nuclear spin order is converted into a large nonequilibrium spin polarization, called hyperpolarization. This hyperpolarization can lead to an enhancement of the NMR signals by more than 3 orders of magnitude.[4] While normal hydrogen (assigned n-H_2 in this work) has a para (spin $I = 0$) to ortho (spin $I = 1$) ratio of 1:3, contact of n-H_2 with activated charcoal or iron oxide at low temperature (e.g., 77 K) is accompanied by conversion to hydrogen with a para:ortho ratio of 1:1, corresponding to a parahydrogen enrichment (assigned p-H_2 in this work).[4,5] In the past decade, PHIP demonstrated a high potential for the investigation of mechanisms of numerous homogeneously catalyzed hydrogenation reactions.[6−13] A very modern field for the application of PHIP is the increase of the NMR detection limit for studies of biological systems and for imaging techniques suitable for applications in medicine.[13−16] Very recently, first in situ continuous-flow MAS NMR spectroscopic studies of the formation of PHIP on noble-metal-containing solids were performed with the aim to develop novel experimental approaches for mechanistic studies in the field of heterogeneous catalysis.[17−19]

Generally, PHIP experiments are performed according to the ALTADENA (Adiabatic Longitudinal Transport After Dissociation Engenders Net Alignment) or the PASADENA (Parahydrogen And Synthesis Allow Dramatically Enhanced Nuclear Alignment) protocol.[4,6,15] In the case of ALTADENA, the hydrogenation reaction with p-H_2 is performed outside the NMR magnet, i.e., in the earth's magnetic field, and subsequently, the hydrogenated reaction products are rapidly moved into the high field of an NMR magnet and detected in this field. In an ALTADENA experiment, multiplet signals of polarized spins with partially inverted signals are observed in the ^{1}H NMR spectrum. In PASADENA experiments, the hydrogenation reaction with p-H_2 is performed in the magnetic field of an NMR spectrometer and also spectroscopically investigated in this field. For PASADENA experiments and pairwise incorporation of p-H_2 into the reactant molecules, antiphase signals occur in the ^{1}H NMR spectra.[4,5,20]

Early PHIP experiments with porous catalysts using the Wilkinson's complex $RhCl(PPh_3)_3$ immobilized, e.g., on

Received: February 27, 2017
Revised: April 10, 2017
Published: April 18, 2017

© 2017 American Chemical Society

DOI: 10.1021/acs.jpcc.7b01899
J. Phys. Chem. C 2017, 121, 9953−9962

SiO_2[5,21] and SBA-15[22] were performed with reactants in the liquid phase. For hydrogenation reactions with the reactants and p-H_2 in the gas phase, catalysts consisting of platinum and palladium supported on Al_2O_3, SiO_2, TiO_2, and ZrO_2[23,24] or the Au(III) Schiff base complex immobilized in a metal−organic framework were utilized.[25] Koptyug and colleagues published a number of very fundamental studies on the PHIP effect on solid hydrogenation catalysts.[23,26−29] Investigating certain noble metals and noble metal oxides in the hydrogenation of 1-butyne with p-H_2, Kovtunov et al. found a better signal enhancement by PHIP on platinum compounds in comparison with palladium compounds.[26] Systematic studies of the hydrogenation of propene with p-H_2 on Pt/Al_2O_3 catalysts with different metal particles sizes demonstrated a much stronger PHIP effect for very small particle sizes ($\phi_{particle}$ < 1 nm) in comparison with larger particle sizes.[23] Furthermore, the reduction of the noble metal compounds on the solid support materials was found to be an important prerequisite for a high formation of PHIP.[27]

In a previous work,[17] we utilized in situ continuous-flow MAS NMR spectroscopy for studying the formation of PHIP by hydrogenating propene with p-H_2 inside the pores of noble metal-containing zeolite Y and SBA-15. Low rhodium loadings of 0.4 wt % ensured the presence of very small metal particles, e.g., 0.5 Rh per unit cell in zeolite Y. In agreement with ref 27, the hydrogenation catalysts were reduced in flowing hydrogen at 653 K for 2 h before the PHIP experiments were performed via the PASADENA protocol. Arzumanov and Stepanov utilized a very similar experimental approach and observed antiphase signals due to the formation of PHIP via the hydrogenation of propene with p-H_2 on Pt/TiO_2 (1 wt % Pt, $\phi_{particle} \cong 1$ nm).[18] Very recently, we demonstrated the advantage of 2D nutation MAS NMR spectroscopy for the separation of antiphase signals caused by the pairwise incorporation of parahydrogen into propene on noble-metal-containing silica (0.9 wt % Pt on SiO_2).[19] This signal separation is reached by utilizing the double nutation frequency of hyperpolarized ^1H nuclei compared to thermally polarized ^1H nuclei.

In the present work, homologous series of porous support materials with different pore sizes (silica, mesoporous SBA-15, dealuminated zeolite Y (DeA−Y), and zeolite H,Na−Y), loaded with same types and numbers of noble metals and of same porous support material (zeolite H,Na−Y), loaded with different noble metals (platinum, rhodium, iridium, and palladium), were investigated in the gas phase hydrogenation of propene with p-H_2. PHIP experiments were performed applying the PASADENA protocol and via in situ MAS NMR spectroscopy under continuous-flow conditions. In comparison with our earlier study,[17] the in situ MAS NMR technique was improved by decreasing the MAS rotor diameter from 7 mm in ref 17 to 4 mm, which allows a higher sample spinning rate. Via in situ MAS NMR spectroscopy of the hydrogenation of acrylonitrile with n-H_2 under semibatch conditions,[30] the hydrogenation activities of the above-mentioned catalysts were investigated. These experiments opened the way for a comparison of intrinsic hydrogenation rates with the PHIP formation properties on the catalysts under study. To the best of our knowledge, the present work is the first systematic investigation of the formation and detection of the hyperpolarized reactants inside micro- and mesopores of solid catalysts with pore sizes of ϕ_{pores} = 0.7−4.5 nm. By this approach, parameters being important for optimizing porous catalysts for future PHIP experiments and studies of heterogeneously catalyzed hydrogenation reactions could be considered.

2. EXPERIMENTAL METHODS

2.1. Sample Preparation. The commercial silica Aerosil 300 (Degussa AG, Hanau, Germany) was used as delivered. The platinum loading of the silica was carried out by stirring 5 g of the silica material in 100 mL of demineralized water at 313 K for 2 h and subsequent addition of 1 M aqueous solution of ammonia until the pH of the solution reached pH = 10. Then, an aqueous solution with calculated amounts of the platinum salt $[Pt(NH_3)_4]Cl_2{\cdot}xH_2O$ (55.66 wt % Pt, ChemPur) or the rhodium salt $RhCl_3{\cdot}xH_2O$ (99.99%, Alfa Aesar) was added dropwise. These solutions were stirred at 313 K for another 18 h. Finally, the solutions were washed with 1.5 L of demineralized water and dried under atmospheric conditions at 353 K for 12 h. The obtained samples with platinum contents of 0.23, 0.50, and 0.85 wt % were assigned 0.2Pt/silica, 0.5Pt/silica, and 0.9Pt/silica, respectively, while the sample with the rhodium content of 0.29 wt % was assigned 0.3Rh/silica.

The mesoporous SBA-15 was synthesized as described by Zhao et al.[31] The as-synthesized SBA-15 was heated with a rate of 2 K/min up to 823 K and calcined in air for 5 h to decompose the template material. Subsequently, an aqueous wetness impregnation with calculated amounts of the platinum salt $[Pt(NH_3)_4]Cl_2{\cdot}xH_2O$ (55.66 wt % Pt, ChemPur) or the rhodium salt $RhCl_3{\cdot}xH_2O$ (99.99%, Alfa Aesar) was performed. After stirring the solutions for 5 min, the water was removed under vacuum at 313 K, and the impregnated catalysts were dried under atmospheric conditions at 353 K for 12 h. The obtained samples were assigned 0.9Pt/SBA-15 and 0.3Rh/SBA-15.

The commercially available dealuminated zeolite DeA-Y with a n_{Si}/n_{Al} ratio of 93 (Degussa AG, Hanau, Germany) and zeolite Na−Y with n_{Si}/n_{Al} = 2.7 (Degussa AG, Hanau, Germany) were purified with 1 M aqueous solution of sodium nitrate at 353 K for 4 h and subsequently washed with demineralized water until all of the nitrate was removed. The purified zeolites DeA−Y and Na−Y were dried under atmospheric conditions at 353 K for 12 h. The noble-metal-containing dealuminated zeolites DeA−Y were prepared by wetness impregnation using the same procedure like for the noble-metal-containing SBA-15, which led to the samples 0.9Pt/DeA−Y and 0.4Rh/DeA−Y.

Zeolites 0.9Pt/H,Na−Y, 0.4Rh/H,Na−Y, 0.8Ir/H,Na−Y, and 0.4Pd/H,Na−Y were obtained by aqueous ion exchange of the above-mentioned purified zeolite Na−Y with a calculated amount of $[Pt(NH_3)_4]Cl_2{\cdot}xH_2O$ (55.66 wt % Pt, ChemPur), $RhCl_3{\cdot}xH_2O$ (99.99%, Alfa Aesar), $[Ir(NH_3)_5Cl]Cl_2$ (99.95%, Sigma-Aldrich), and $[Pd(NH_3)_4]Cl_2{\cdot}xH_2O$ (40.62 wt % Pd, ChemPur), respectively, as described in ref 32. Calcination and reduction of the noble-metal-containing zeolite Na−Y led to the formation of 0.1 to 0.3 Brønsted acidic bridging OH groups (Si(OH)Al) per unit cell.[32]

All noble-metal-containing catalysts were calcined in synthetic air (750 mL/min) by heating with a rate of 2 K/min up to 573 K and calcination at this temperature for 3 h. Before the hydrogenation experiments, the noble-metal-containing catalysts under study were dehydrated and reduced in flowing hydrogen (100 mL/min) at 623 K for 2 h, transferred into glass tubes inside a glovebox under a nitrogen

DOI: 10.1021/acs.jpcc.7b01899
J. Phys. Chem. C 2017, 121, 9953−9962

Table 1. Sample Assignments, Silicon to Aluminum Ratios, Noble Metal Contents, Noble Metal Dispersions, *D*, Specific BET Surface Areas, Total Pore Volumes, and Pore Sizes of the Noble-Metal-Containing Catalysts under Study

catalyst	n_{Si}/n_{Al} [a]	noble metal content[a] (wt %)	D[b] (%)	BET surface[c] ($m^2\ g^{-1}$)	total pore volume ($cm^3\ g^{-1}$)	pore size (nm)
0.9Pt/silica	∞	0.85	83	277	0.31	4.55[c]
0.9Pt/SBA-15	199	0.78	68	420	0.36	3.43[c]
0.9Pt/DeA−Y	93	0.96	72	721	0.42	0.74[d]
0.9Pt/H,Na−Y	2.7	0.82	73	937	0.47	0.74[d]
0.3Rh/silica	∞	0.29	59	282	0.27	3.77[c]
0.3Rh/SBA-15	209	0.33	60	690	0.72	4.07[c]
0.4Rh/DeA−Y	112	0.37	68	749	0.39	0.74[d]
0.4Rh/H,Na−Y	2.7	0.42	63	1012	0.54	0.74[d]
0.8Ir/H,Na−Y	2.7	0.84	121	1050	0.52	0.74[d]
0.4Pd/H,Na−Y	3.0	0.40	43	913	0.45	0.74[d]

[a]Determined by chemical analysis using ICP-OES with an accuracy of ±10%. [b]Dispersion, *D*, determined by H_2 chemisorption assuming a stoichiometry of 1 H atom per noble metal atom.[38,39] [c]Average pore diameter determined by N_2 physisorption.[40] [d]Crystallographic pore diameter of the FAU structure of zeolite Y.[44]

atmosphere, and, subsequently, evacuated ($p < 10^{-2}$ Pa) at 298 K for 12 h.

2.2. Characterization Methods. The chemical compositions of the noble-metal-containing catalysts under study were determined by optical emission spectroscopy (ICP-OES, Varian Vista-MPX). The structural intactness was proved by XRD (Bruker D8 diffractometer) and via ^{27}Al and ^{29}Si solid-state NMR spectroscopy (Bruker AVANCE III 400WB). The BET surface areas were measured by physisorption of nitrogen (Autosorb-1 of Quantachrome), while the metal dispersion was investigated by chemisorption of hydrogen using the same equipment.

2.3. In Situ Solid-State NMR Spectroscopy. All in situ ^{1}H MAS NMR experiments were performed with a Bruker AVANCE III 400WB spectrometer, using a 4 mm Bruker MAS NMR probe, modified as described in the literature,[17,33−35] at the resonance frequency of 400.13 MHz and after single-pulse excitation. The 4 mm Bruker MAS NMR rotors were utilized with DELRIN caps, which have a hole of 1.2 mm in the middle. To inject hydrogen gas or the reactant mixture into the spinning 4 mm MAS NMR rotor, a glass tube with an outer diameter of 1 mm was inserted into the sample volume of the rotor via the 1.2 mm hole in the cap (see Figure S1 in Supporting Information). An empty space, shaped like a hollow cylinder with an inner diameter of ca. 1.2 mm inside the rotor filled with the catalyst, ensured that no mechanical contact between the fixed injection tube and the rotating catalyst existed.

The in situ ^{1}H MAS NMR studies of the hydrogenation of acrylonitrile were performed under semibatch conditions and with n-H_2 (ortho to para ratio of 3:1). Before the experiments, 50 ± 5 mg of dehydrated and reduced catalyst, filled into a 4 mm Bruker MAS NMR rotor, was loaded with acrylonitrile (natural abundance of isotopes, Acros Organics, purity of 99.9%) at a vacuum line. To remove physisorbed acrylonitrile, the sample were evacuated at 298 K for 10 min. Subsequently, the rotor containing the acrylonitrile-loaded catalyst was sealed with a common rotor cap to control the acrylonitrile loading. The amount of the adsorbed acrylonitrile was determined by ^{1}H MAS NMR spectroscopy using $\pi/2$ single-pulse excitation and a repetition time of 20 s.

For the in situ ^{1}H MAS NMR studies of the acrylonitrile hydrogenation, a 4 mm Bruker MAS NMR rotor with modified rotor cap was used. By spinning the catalyst-filled rotor at 8 kHz for 10 min, the catalyst powder was pressed to a cylindrical catalyst bed (see Figure S1). After insertion of the glass tube for the injection of the n-H_2 and stabilization of the temperature at 298 K, the first single-scan ^{1}H MAS NMR spectrum was recorded 4 s after starting the n-H_2 injection with a flow of 300 mL/min into the rotor during spinning the catalyst with 4 kHz, while the subsequent single-scan spectra were recorded every 10 s. The signal intensities were evaluated by comparing with an external intensity standard (dehydrated zeolite 35H,Na−Y) after the in situ experiments and by simulating the spectra using the Bruker software WinFit.

The hydrogenation of propene (Westfalen AG, Munster, Germany, purity of 99.5%) with p-H_2 (para to ortho ratio of 1:1) was performed under continuous-flow conditions for both reactants. The p-H_2 enrichment was performed by partial conversion of the orthohydrogen in the common hydrogen (Westfalen AG, Munster, Germany, purity of 99.999%) at an FeO(OH) catalyst (Sigma-Aldrich) cooled to 77 K. The propene and p-H_2 gas flows were adjusted via Swagelok needle valves and a rotameter (see Figure S2).

Prior to the in situ ^{1}H MAS NMR investigations of the propene hydrogenation, 40 ± 5 mg of dehydrated and reduced catalyst was loosely filled into a 4 mm Bruker MAS NMR rotor, inside a glovebox purged with dry nitrogen gas. By spinning this powder with 8 kHz for 10 min, it was pressed to a cylindrical catalyst bed allowing the insertion of the tube for the injection of the reactant mixture. The in situ ^{1}H MAS NMR spectra were recorded at 373 K upon $\pi/4$ single-pulse excitation, with 512 scans per spectrum, a repetition time of 0.1 s, at a spinning rate of ca. 4 kHz, and with propene and p-H_2 flow rates of 40 and 30 mL/min, respectively. Before, it was evidenced that no saturation occurs for continuous-flow ^{1}H MAS NMR experiments with the repetition time of 0.1 s. The ^{1}H MAS NMR signal intensities were evaluated by comparison with the spectra obtained during propene hydrogenation with n-H_2 and integration with the software module SOLA of TopSpin 3.5.

3. RESULTS AND DISCUSSION

3.1. Physical Properties of the Catalysts under Study. An overview on the assignments of the catalysts under study, their n_{Si}/n_{Al} ratios, and the noble metal contents, determined by ICP/OES, are given in Table 1, columns 1−3. The aluminum contents of the silica, SBA-15, and zeolite DeA−Y correspond to those of siliceous supports. The n_{Si}/n_{Al} ratios of the catalysts containing zeolite H,Na−Y as support material do not show significant differences. By solid-state NMR spectroscopy was

DOI: 10.1021/acs.jpcc.7b01899
J. Phys. Chem. C 2017, 121, 9953−9962

Table 2. Sample Assignments, Loadings of Acrylonitrile on the Noble-Metal-Containing Catalysts under Study, Velocity Rate Constants, k, and Reaction Rates, r, of the Hydrogenation of Acrylonitrile under Semibatch Conditions at 298 K, Determined by In Situ ^{1}H MAS NMR Spectroscopy

catalyst	acrylonitrile[a] (mmol)	k (s^{-1})	r (mmol s^{-1})
0.9Pt/silica	0.023	$(3.3 \pm 0.3) \times 10^{-2}$	$(7.6 \pm 1.1) \times 10^{-4}$
0.9Pt/SBA-15	0.018	$(1.8 \pm 0.2) \times 10^{-2}$	$(3.2 \pm 0.5) \times 10^{-4}$
0.9Pt/DeA−Y	0.018	$(3.8 \pm 0.4) \times 10^{-2}$	$(6.8 \pm 0.9) \times 10^{-4}$
0.9Pt/H,Na−Y[b]	0.021	$(1.1 \pm 0.1) \times 10^{-2}$	$(2.3 \pm 0.3) \times 10^{-4}$
0.3Rh/silica	0.022	$(2.4 \pm 0.2) \times 10^{-2}$	$(5.3 \pm 0.7) \times 10^{-4}$
0.3Rh/SBA-15	0.020	$(4.6 \pm 0.5) \times 10^{-2}$	$(9.1 \pm 1.3) \times 10^{-4}$
0.4Rh/DeA−Y	0.020	$(1.2 \pm 0.1) \times 10^{-1}$	$(24 \pm 4) \times 10^{-4}$
0.4Rh/H,Na−Y[b]	0.020	$(3.4 \pm 0.3) \times 10^{-2}$	$(6.8 \pm 1.0) \times 10^{-4}$
0.8Ir/H,Na−Y[b]	0.017	$(6.7 \pm 0.7) \times 10^{-4}$	$(0.11 \pm 0.02) \times 10^{-4}$
0.4Pd/H,Na−Y[b]	0.027	1.1 ± 0.3	$(270 \pm 50) \times 10^{-4}$

[a]Determined by ^{1}H MAS NMR with an accuracy of ±5%. [b]Data are taken from ref 45.

evidenced that the corresponding aluminum atoms are tetrahedrally coordinated framework species (not shown).

The noble metal loadings were calculated and performed in such a manner that the same number of metal atoms per gram catalyst exists on the catalysts, independent of the weight of the noble metal, excluding for the samples 0.2Pt/silica and 0.5Pt/silica mentioned in section 2.1. For zeolites Y, these noble metal loadings correspond to 0.50 ± 0.05 metal atoms per unit cell. The noble metal dispersions, D, given in Table 1, column 4, are in the range of 59−83%, which are typical values for similar catalysts in the literature.[36,37] These noble metal dispersions were calculated assuming a stoichiometry of 1 H atom per noble metal atom.[38,39] Only for zeolites 0.8Ir/H,Na−Y (D = 121%) and 0.4Pd/H,Na−Y (D = 43%), strong deviations in the noble metal dispersions, D, were observed, which may be due to different chemisorption stoichiometries, at least for the iridium-containing catalyst. In a similar manner, the metal particle diameters, calculated by the hydrogen chemisorption data, are in the narrow range of 1.4−1.7 nm, excluding for the metal particle diameters of zeolites 0.8Ir/H,Na−Y (0.8 nm) and 0.4Pd/H,Na−Y (2.6 nm).

The specific surface areas of the samples under study in column 5 of Table 1, determined via the method of Brunauer, Emmett, and Teller,[40] are typical for similar materials described in the literature.[41−43] The slightly lower value for zeolite 0.9Pt/DeA−Y compared with zeolite 0.9Pt/H,Na−Y is caused by the dealumination procedure applied to zeolite DeA−Y. Similarly, also the total pore volumes in column 6 of Table 1 reflect typical adsorption properties of the mesoporous and microporous supports utilized in the present work. These pore volumes are in the range of 0.31−0.56 $cm^3\ g^{-1}$ with the larger values for the zeolites Y under study. The pore diameters summarized in column 7 of Table 1 were calculated via the nitrogen adsorption data for the samples 0.9Pt/silica and 0.9Pt/SBA-15 or correspond to the crystallographic pore diameters of the FAU structure for all zeolites Y under study.[44]

3.2. In Situ MAS NMR Investigation of the Hydrogenation Activity of the Noble-Metal-Containing Catalysts under Study. In situ ^{1}H MAS NMR spectroscopy of the hydrogenation of acrylonitrile under semibatch conditions was performed for investigating the intrinsic hydrogenation activity of the homologous series of Pt- and Rh-containing solid catalysts with different porosities.[45] For this purpose, three siliceous supports, i.e., silica (ϕ_{pore} = 4.5 nm), mesoporous SBA-15 (ϕ_{pore} = 3.4 nm), and dealuminated zeolite DeA−Y (ϕ_{pore} = 0.7 nm), with a similar platinum loading (lines 2−5 in Table 1) were used. For comparison, also a Pt- and Rh-containing aluminum-rich zeolite H,Na−Y (n_{Si}/n_{Al} = 2.7) was investigated. Before the in situ ^{1}H MAS NMR experiments, the dehydrated and reduced catalysts were loaded with acrylonitrile according to column 2 of Table 2. Subsequently, the acrylonitrile-loaded samples were transferred into the spectrometer, and the hydrogenation was spectroscopically observed as a function of time, after starting the hydrogen flow, and at the temperature of 298 ± 1 K.

The kinetics of the acrylonitrile hydrogenation were determined via the time-dependent changes of the ^{1}H MAS NMR signals of the CH_2 (6.1 ± 0.2 ppm) and CH groups (5.7 ± 0.2 ppm) of acrylonitrile and the CH_3 (1.0 ± 0.3 ppm) and CH_2 groups (2.2 ± 0.2 ppm) of propionitrile. Slight deviations of the experimentally observed shift values in comparison with the reference values determined in the liquid phase (see Scheme 1a)[46] are due to adsorption effects. As an example,

Scheme 1. Survey on the ^{1}H NMR Shift Values, δ_{1H}, of the Reactants Contributing to the Hydrogenation of Acrylonitrile (Top) and Propene (Bottom) on Noble-Metal-Containing Catalysts, According to Ref 46

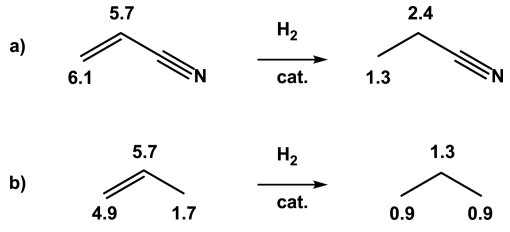


Figure 1 shows the stack plot of in situ ^{1}H MAS NMR spectra recorded during the hydrogenation of acrylonitrile on 0.9Pt/silica up to the reaction time of 84 s.

For determining the velocity rate constants, k, of the acrylonitrile hydrogenation, the time-dependent intensities $I(t)$ of the ^{1}H MAS NMR signals of acrylonitrile were evaluated by a quantitative simulation of the recorded spectra. Subsequently, the negative logarithms of the intensities $I(t)$, related to the intensities I_0 of the ^{1}H MAS NMR signals of acrylonitrile before starting the hydrogen flow, were plotted as a function of the reaction time t. As an example, Figure 2 shows the plots of the $-\ln(I(t)/I_0)$ values as a function of the reaction time for the acrylonitrile hydrogenation on 0.9Pt/silica, 0.9Pt/SBA-15, 0.9Pt/DeA−Y, and 0.9Pt/H,Na−Y.

DOI: 10.1021/acs.jpcc.7b01899
J. Phys. Chem. C 2017, 121, 9953−9962

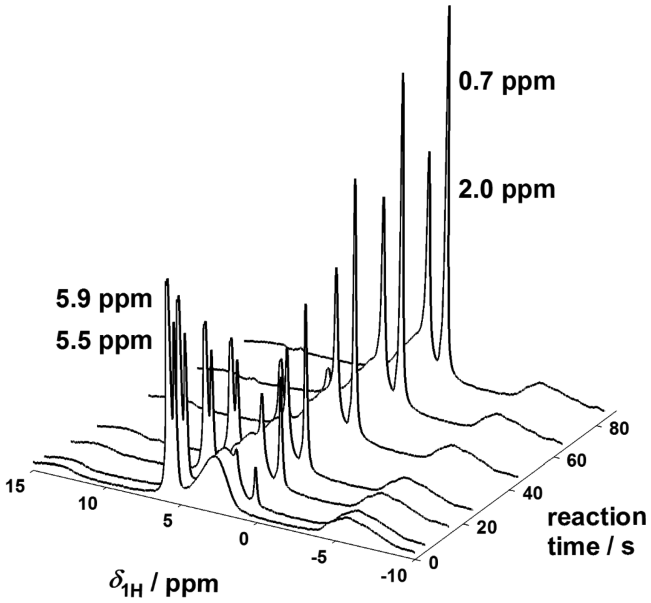


Figure 1. Stack plot of in situ ^{1}H MAS NMR spectra recorded during the hydrogenation of acrylonitrile on platinum-containing (0.9 wt %) silica (0.9Pt/silica) under semibatch conditions at 298 K.

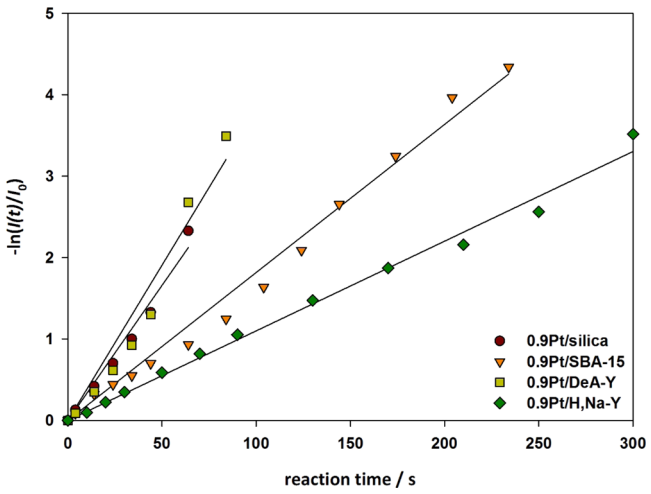


Figure 2. Negative logarithms of the intensity ratios $I(t)/I_0$ of the ^{1}H MAS NMR signals of acrylonitrile plotted as a function of the reaction time, t, for the hydrogenation of acrylonitrile on platinum-containing (0.9 wt %) silica, SBA-15, dealuminated zeolite DeA−Y, and zeolite H,Na−Y under semibatch conditions at 298 K. The value I_0 corresponds to the signal intensity at t = 0.

The obtained k values, determined by the slope of a linear regression (least-squares fitted) passing through the coordinate origin, are summarized in column 3 of Table 2, lines 2−5. Via the same procedure, the in situ ^{1}H MAS NMR spectra recorded during the hydrogenation of acrylonitrile on the Rh-containing catalysts were evaluated. Using the acrylonitrile loadings given in column 2 of Table 2, the reaction rates, r, summarized in column 4 were calculated. Interestingly, the reaction rates of the Pt- and Rh-containing siliceous catalysts are in the range of r = 3×10^{-4} to 8×10^{-4} mmol s^{-1} and $r = 5 \times 10^{-4}$ to 24×10^{-4} mmol s^{-1}, respectively. Hence, the intrinsic hydrogenation rates of 0.9 wt % Pt or 0.3−0.4 wt % Rh on silica, SBA-15, and zeolite DeA−Y are similar, i.e., almost independent of the very different pore sizes of these catalysts. Furthermore, also the dealuminated zeolite DeA−Y (n_{Si}/n_{Al} = 93) and zeolite H,Na−Y (n_{Si}/n_{Al} = 2.7) with same pore size and 0.9 wt % Pt and 0.4 wt % Rh show intrinsic hydrogenation rates in a narrow range of $r = 2 \times 10^{-4}$ to 7×10^{-4} mmol s^{-1} and $r = 7 \times 10^{-4}$ to 24×10^{-4} mmol s^{-1}, respectively. Hence, also the effect of the different aluminum contents (n_{Si}/n_{Al} ratios) of these zeolite catalysts on their hydrogenation activity was found to be weak. In this connection should be mentioned that the same number of different noble metal atoms, such as Pt, Rh, Ir, and Pd, loaded on the same support (zeolite H,Na−Y) leads to activities in the hydrogenation of acrylonitrile, which vary over 4 orders of magnitude (Table 2, lines 5 and 9−11).

3.3. Effect of Reaction Temperature and Application of MAS on the Antiphase Signals Caused by Hydrogenation of Propene with p-H$_2$. Until now, PHIP experiments with reactants in the gas phase were performed with static samples, i.e., without application of MAS, excluding in our earlier work and in the work of Arzumanov and Stepanov.[17−19] In the present work, the reactants are mainly located inside the catalyst pores during their NMR detection. The pore volumes of all samples under study are in the narrow range of 0.31−0.56 cm^3 g^{-1} (Table 1, column 6). In contrast to our earlier work,[17] the content of empty sample volume inside the catalyst-filled MAS rotors used in the present work is much lower (<20%) and mainly purged by propene and p-H$_2$ before first contact with the catalyst (volume of injection tube). The steric limitations of the catalyst pores restrict the mobility of the reactant molecules after their adsorption, which causes a broadening of their NMR signals. This signal broadening is due to the anisotropy of the chemical shielding and dipolar interactions, which can be averaged by application of MAS. For demonstrating the line-narrowing effect of MAS, Figures 3a and 3b show in situ ^{1}H solid-state NMR spectra recorded during the hydrogenation of propene with p-H$_2$ on 0.9Pt/silica at 298 K without MAS and with MAS, respectively. The difference spectra shown at bottom of Figures 3a and 3b demonstrate that application of MAS causes a significant narrowing of the antiphase signals at 0.8 to 1.6 ppm, which are due to the pairwise incorporation of p-H$_2$ into propene (see Scheme 1b). This observation also indicates that the hyperpolarized reaction products of the hydrogenation of propene with p-H$_2$ are located inside catalyst pores, and it hints at significant spin interactions of the product molecules with nuclei in the pore walls of the host materials.

Furthermore, the effect of the temperature during the in situ ^{1}H MAS NMR spectroscopic studies of the hydrogenation of propene with p-H$_2$ was investigated. For this purpose, Figures 3b and 3c, bottom, show the antiphase signals obtained during hydrogenation of propene with p-H$_2$ on 0.9Pt/silica at 298 and 373 K, respectively. An additional, but very weak line narrowing occurs in the in situ ^{1}H MAS NMR spectrum recorded at 373 K in comparison with that obtained at 298 K. Similar observations were made for the in situ ^{1}H MAS NMR spectra recorded during hydrogenation of propene with p-H$_2$ on 0.9Pt/SBA-15, 0.9Pt/DeA−Y, and 0.9Pt/H,Na−Y. In the investigated temperature range of 298−373 K, most of the spin interactions responsible for a broadening of the reactant signals are averaged by MAS, while the thermal mobility of the reactant molecules has only a minor effect on the signal shape. On the other hand, since an elevated temperature during the propene hydrogenation should have a positive effect on the pore diffusion and desorption of the reactant molecules, all subsequent in situ ^{1}H MAS NMR studies were performed at 373 K.

DOI: 10.1021/acs.jpcc.7b01899
J. Phys. Chem. C 2017, 121, 9953−9962

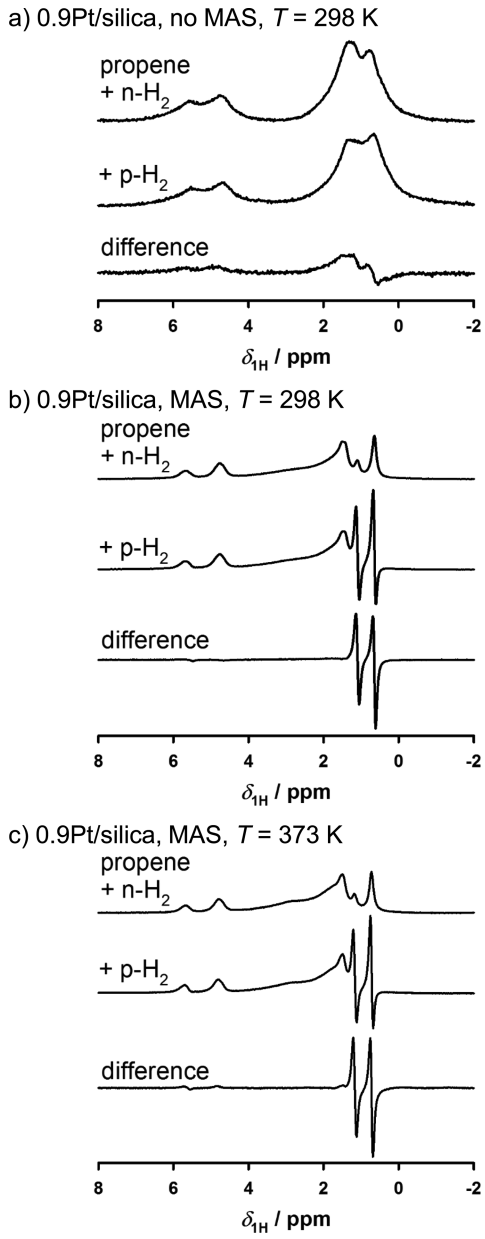


Figure 3. In situ ^{1}H solid-state NMR spectra recorded during the hydrogenation of propene with n-H_2 (top) and p-H_2 (middle) on platinum-containing (0.9 wt %) silica (0.9Pt/silica) under continuous-flow conditions at 298 K without MAS (a), at 298 K with MAS (b), and at 373 K with MAS (c). The bottom spectra are the difference of the spectra recorded during hydrogenation with n-H_2 and p-H_2.

3.4. Effect of the Catalyst Pore Size and Aluminum Content on the Antiphase Signals Caused by Hydrogenation of Propene with p-H_2. Strong antiphase signals, caused by the pairwise incorporation of p-H_2 into propene, require a slow relaxation of the hyperpolarized ^{1}H nuclei of the product molecules. For these relaxation processes, spin interactions of the product molecules with nuclei in the pore walls are responsible. Therefore, quantitative studies of the antiphase signals during the propene hydrogenation on solid catalysts with different pore sizes and different aluminum contents were performed. For this purpose, two homologous series of Pt- (0.9 wt %) and Rh-containing (0.4 wt %) silica, mesoporous SBA-15, dealuminated zeolite DeA−Y, and zeolite H,Na−Y were investigated during the hydrogenation of propene with p-H_2. The in situ ^{1}H MAS NMR difference spectra recorded during the hydrogenation of propene with p-H_2 on these catalysts are shown in Figures 4a−d and 5a−d.

All antiphase signals shown on the left-hand side of Figures 4 and 5 have same signal shapes and positions, but strongly different intensities. These signals were obtained under identical conditions of the propene hydrogenation, since same optimized reactant flows (propene, p-H_2) led to optimum signal intensities for all catalyst under study (see section 2.3). Table 3, lines 4−11, give a survey on the relative intensities of the antiphase signals, determined by comparing the intensities of the in situ ^{1}H MAS NMR spectra recorded during propene hydrogenation with n-H_2 and p-H_2. In Figures 4e and 5e, these relative intensities of the antiphase signals are plotted as a function of the pore diameters (Table 1, column 7).

For clarifying the effect of the amount of same noble metals on the experimental results, the platinum loading on silica was varied between 0.2 and 0.9 wt % (0.2Pt/silica, 0.5Pt/silica, and 0.9Pt/silica). In situ ^{1}H MAS NMR spectroscopy during the hydrogenation of propene with p-H_2 led to a less significant change of the intensity of the antiphase signals (Table 3, lines 2−4) than observed upon variation of the support material, such as observed for 0.9Pt/silica, 0.9Pt/SBA-15, and 0.9Pt/DeA−Y (see Table 3, lines 4−6). Hence, the amount of the noble metal loading is the less critical parameter for optimizing the intensities of the antiphase signals in comparison with the morphology of the catalyst support.

The plots of the antiphase signal intensities as a function of the pore diameters, ϕ_{pores}, in Figures 4e and 5e, hint at their obvious dependence on the type of the platinum- and rhodium-containing siliceous supports, i.e., silica, SBA-15, and zeolite DeA−Y. Hydrogenation of propene with p-H_2 on noble-metal-containing catalysts with larger pores, such as silica, led to larger antiphase signals than on noble-metal-containing catalysts with smaller pores, such as SBA-15 and zeolite DeA−Y. This is a clear evidence for an enhanced relaxation of the hyperpolarized propane molecules inside small pores and vice versa. Furthermore, the antiphase signals recorded during the hydrogenation of propene by p-H_2 on noble-metal-containing zeolites DeA−Y (n_{Si}/n_{Al} = 93) and H,Na−Y (n_{Si}/n_{Al} = 2.7) are compared in Figures 4e and 5e. Obviously, a significantly smaller antiphase signal occurs in the case of zeolite H,Na−Y with the much higher aluminum content but same pore size. This observation indicates a significantly enhanced relaxation of the hyperpolarized propane by spin interactions with framework aluminum species (spin I = 5/2) and extra-framework sodium cations (spin I = 3/2) inside the pores of zeolite H,Na−Y.

On the other hand, no correlation between the antiphase signal intensities and the intrinsic hydrogenation activities, r, of the Pt- and Rh-containing catalysts could be found, which may be due to the narrow range of r values in these cases (Table 2, column 4).

3.5. Pairwise Incorporation of p-H_2 into Propene on Zeolite H,Na−Y Loaded with Platinum, Rhodium, Iridium, and Palladium. The in situ ^{1}H MAS NMR spectroscopic study of the acrylonitrile hydrogenation on zeolite H,Na−Y loaded with different noble metals led to reaction rates, r, covering a range of 4 orders of magnitude (section 3.2). Therefore, it was interesting to investigate the effect of these very different hydrogenation activities on the formation of hyperpolarized propane being responsible for the occurrence of antiphase signals in the ^{1}H MAS NMR spectra.

DOI: 10.1021/acs.jpcc.7b01899
J. Phys. Chem. C 2017, 121, 9953−9962

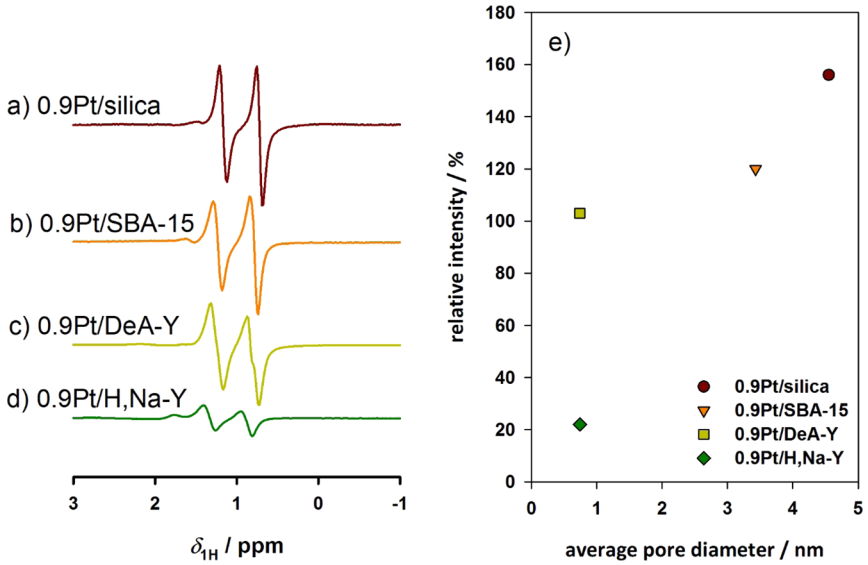


Figure 4. In situ ^{1}H MAS NMR antiphase signals observed during hydrogenation of propene with p-H_2 on platinum-containing (0.9 wt %) silica (a), SBA-15 (b), dealuminated zeolite DeA−Y (c), and zeolite H,Na−Y (d). (e) Plot of their relative intensities as a function of the pore diameters, ϕ_{pores}, of the above-mentioned porous support materials.

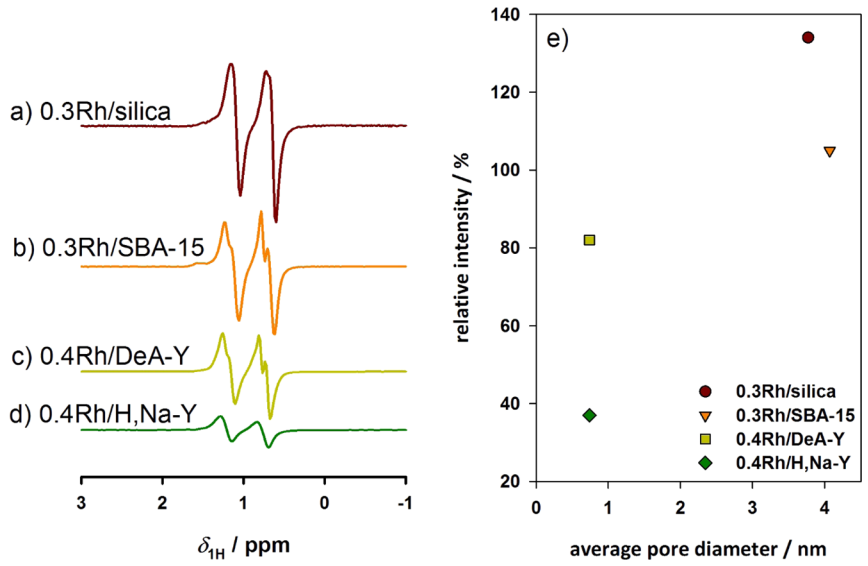


Figure 5. In situ ^{1}H MAS NMR antiphase signals observed during hydrogenation of propene with p-H_2 on rhodium-containing (0.3−0.4 wt %) silica (a), SBA-15 (b), dealuminated zeolite DeA−Y (c), and zeolite H,Na−Y (d). (e) Plot of their relative intensities as a function of the pore diameters, ϕ_{pores}, of the above-mentioned porous support materials.

Table 3. Relative Intensities of the ^{1}H MAS NMR Antiphase Signals Caused by Hydrogenation of Propene with Parahydrogen (p-H_2) under Continuous-Flow Conditions at 373 K at the Noble-Metal-Containing Catalysts under Study

catalyst	rel int[a] (%)	catalyst	rel int[a] (%)
0.2Pt/silica	129	0.3Rh/silica	134
0.5Pt/silica	151	0.3Rh/SBA-15	105
0.9Pt/silica	156	0.4Rh/DeA−Y	82
0.9Pt/SBA-15	120	0.4Rh/H,Na−Y	37
0.9Pt/DeA−Y	103	0.8Ir/H,Na−Y	7
0.9Pt/H,Na−Y	22	0.4Pd/H,Na−Y	4

[a]Determined by ^{1}H MAS NMR spectroscopy with an accuracy of ±5% using the total intensity of the spectra obtained by hydrogenation of propene with normal hydrogen (n-H_2).

Figures 6a−d show the in situ ^{1}H MAS NMR difference spectra recorded during the hydrogenation of propene with p-H_2. Figure 6e is the plot of the relative intensities of the antiphase signals, caused by the pairwise incorporation of p-H_2 into propene, as a function of the reaction rate, *r*, for the acrylonitrile hydrogenation (Table 2, column 4). For zeolites 0.8Ir/H,Na−Y, 0.9Pt/H,Na−Y, and 0.4Rh/H,Na−Y, an obvious increase of the relative intensity of the antiphase signals with increasing hydrogenation rate, *r*, occurs. Hence, suitable catalysts for the formation of hyperpolarized propane by a pairwise incorporation of p-H_2 into propene should have a high hydrogenation activity. On the other hand, for zeolite 0.4Pd/H,Na−Y with the strongly higher hydrogenation rate (Table 2, column 4), only very weak antiphase signals occurred. This finding indicates that noble metal catalysts with a too high hydrogenation activity are not suitable for the formation of

DOI: 10.1021/acs.jpcc.7b01899
J. Phys. Chem. C 2017, 121, 9953−9962

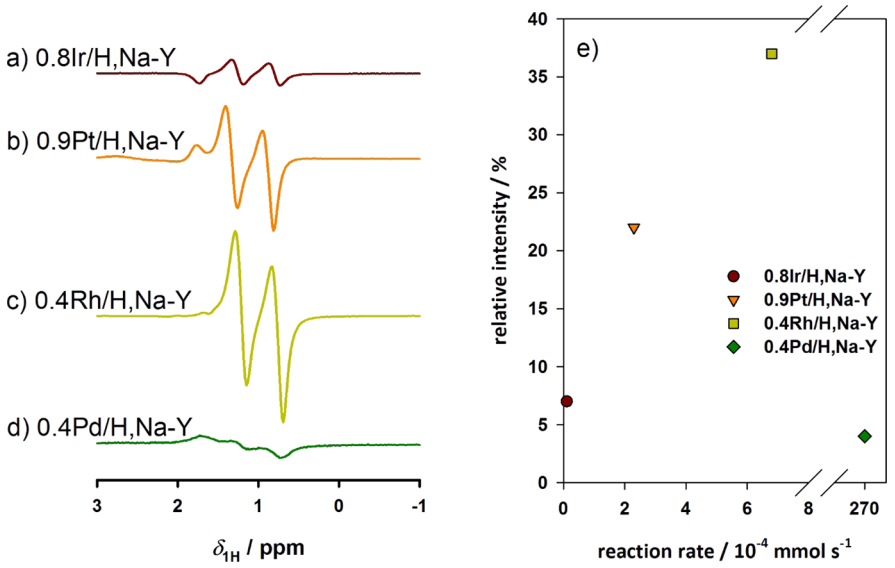


Figure 6. In situ ^{1}H MAS NMR antiphase signals observed during hydrogenation of propene with p-H_2 on zeolite H,Na−Y loaded with iridium (a), platinum (b), rhodium (c), and palladium (d). (e) Plot of their relative intensities as a function of the reaction rates, *r*, in the acrylonitrile hydrogenation at the same catalysts.

PHIP. In this case, probably, too many reactive H species are formed, which hinder the pairwise incorporation of the p-H_2 molecules into propene.

4. CONCLUSIONS

In the present work, homologous series of porous support materials (silica, SBA-15, dealuminated zeolite DeA−Y (n_{Si}/n_{Al} = 93), and zeolite H,Na−Y (n_{Si}/n_{Al} = 2.7)) with different pore sizes (ϕ_{pore} = 4.5−0.7 nm), loaded with same types and numbers of noble metals, and of same support material (zeolite H,Na−Y), loaded with different noble metals (Pt, Rh, Ir, Pd), were applied as catalysts in the gas phase hydrogenation of propene with para-enriched hydrogen (p-H_2) to produce parahydrogen-induced polarization (PHIP). The formation of hyperpolarized propane by a pairwise incorporation of p-H_2 into propene was investigated via in situ ^{1}H MAS NMR spectroscopy under continuous-flow conditions and evaluated via the characteristic ^{1}H NMR antiphase signals of propane, i.e., the hyperpolarized product molecules. The aim of this work was the investigation of experimental parameters and properties of noble-metal-containing porous solid catalysts being important for the formation of PHIP.

Quantitative investigations of the ^{1}H NMR antiphase signals caused by the hydrogenation of propene with p-H_2 on noble-metal-containing siliceous catalysts with different pore sizes indicated an enhanced relaxation of hyperpolarized reactant molecules inside small pores, such as inside the micropores of dealuminated zeolite DeA−Y (ϕ_{pore} = 0.7 nm) compared with those inside the mesopores of siliceous SBA-15 (ϕ_{pore} = 3.4 nm) and silica (ϕ_{pore} = 4.5 nm). In the case of hyperpolarized reactant molecules inside the micropores of zeolite H,Na−Y with n_{Si}/n_{Al} = 2.7, spin interactions with framework aluminum species (spin I = 5/2) and extra-framework sodium cations (spin I = 3/2) caused a significantly enhanced relaxation of the hyperpolarized reactant, corresponding to smaller ^{1}H NMR antiphase signals compared with those inside the pores of dealuminated zeolite DeA−Y with n_{Si}/n_{Al} = 93.

Comparison of solid catalysts with an identical pore size, such as zeolites H,Na−Y loaded with iridium, platinum, and rhodium, hints at a correlation between their reaction rates in the hydrogenation of acrylonitrile ($(0.1-7) \times 10^{-4}$ mmol s^{-1}) and the formation of PHIP by the hydrogenation of propene inside the pores of these catalysts. On the other hand, for the palladium-containing zeolite H,Na−Y with a some orders higher acrylonitrile hydrogenation activity (270×10^{-4} mmol s^{-1}), only very weak ^{1}H MAS NMR antiphase signals were observed. This finding indicates that no pairwise incorporation of p-H_2 into the olefinic reactant molecules can occur in the case of too active hydrogenation catalysts. A possible reason for this observation could be a too large number of reactive spillover H species without any spin correlation on these catalysts.

■ ASSOCIATED CONTENT

Supporting Information

The Supporting Information is available free of charge on the ACS Publications website at DOI: 10.1021/acs.jpcc.7b01899.

Additional information on the experimental setup utilized for the in situ flow MAS NMR investigations (PDF)

■ AUTHOR INFORMATION

Corresponding Author

*E-mail: michael.hunger@itc.uni-stuttgart.de (M.H.).

ORCID

Michael Hunger: 0000-0002-1870-2743

Notes

The authors declare no competing financial interest.

■ ACKNOWLEDGMENTS

We thank Deutsche Forschungsgemeinschaft for financial support (project HU533/13-1) and Matthias Scheibe and Heike Fingerle (both University of Stuttgart) for nitrogen adsorption studies, chemisorption experiments, and ICP-OES measurements.

DOI: 10.1021/acs.jpcc.7b01899
J. Phys. Chem. C 2017, 121, 9953−9962

REFERENCES

(1) Griffin, R. G.; Prisner, T. F. High Field Dynamic Nuclear Polarization − The Renaissance. *Phys. Chem. Chem. Phys.* **2010**, *12*, 5737−5740.

(2) Bowers, C. R.; Weitekamp, D. P. Transformation of Symmetrization Order to Nuclear-Spin Magnetization by Chemical Reaction and Nuclear Magnetic Resonance. *Phys. Rev. Lett.* **1986**, *57*, 2645−2648.

(3) Bowers, C. R.; Weitekamp, D. P. Parahydrogen and Synthesis Allow Dramatically Enhanced Nuclear Alignment. *J. Am. Chem. Soc.* **1987**, *109*, 5541−5542.

(4) Natterer, J.; Bargon, J. Parahydrogen Induced Polarization. *Prog. Nucl. Magn. Reson. Spectrosc.* **1997**, *31*, 293−315.

(5) Skovpin, I. V.; Zhivonitko, V. V.; Koptyug, I. V. Parahydrogen-Induced Polarization in Heterogeneous Hydrogenations over Silica-Immobilized Rh Complexes. *Appl. Magn. Reson.* **2011**, *41*, 393−410.

(6) Duckett, S. B.; Wood, N. J. Parahydrogen-Based NMR Methods as a Mechanistic Probe in Inorganic Chemistry. *Coord. Chem. Rev.* **2008**, *252*, 2278−2291.

(7) Harthun, A.; Selke, R.; Bargon, J. Proof of a Reversible, Pairwise Hydrogen Transfer during the Homogeneously Rhodium(I)-Catalyzed Hydrogenation of α,β-Unsaturated Carbonic Acid Derivatives with In Situ NMR Spectroscopy and Parahydrogen. *Angew. Chem., Int. Ed. Engl.* **1996**, *35*, 2505−2507.

(8) Duckett, S. B.; Sleigh, C. J. Applications of the Parahydrogen Phenomenon: A Chemical Perspective. *Prog. Nucl. Magn. Reson. Spectrosc.* **1999**, *34*, 71−92.

(9) Gutmann, T.; Sellin, M.; Breitzke, H.; Stark, A.; Buntkowsky, G. Para-Hydrogen Induced Polarization in Homogeneous Phase − An Example of How Ionic Liquids Affect Homogenization and Thus Activation of Catalyst. *Phys. Chem. Chem. Phys.* **2009**, *11*, 9170−9175.

(10) Kuhn, L. T.; Bommerich, U.; Bargon, J. Transfer of Parahydrogen-Induced Hyperpolarization to ^{19}F. *J. Phys. Chem. A* **2006**, *110*, 3521−3526.

(11) Stephan, M.; Kohlmann, O.; Niessen, H. G.; Eichhorn, A.; Bargon, J. ^{13}C PHIP NMR Spectra and Polarization Transfer During the Homogeneous Hydrogenation of Alkynes with Parahydrogen. *Magn. Reson. Chem.* **2002**, *40*, 157−160.

(12) Buljubasich, L.; Franzoni, M. B.; Munnemann, K. Parahydrogen-Induced Polarization by Homogeneous Catalysis: Theory and Applications. In *Topics in Current Chemistry: Hyperpolarization Methods in NMR Spectroscopy*; Kuhn, L. T., Ed.; Springer-Verlag: Berlin, 2013, Vol. *338*, pp 33−74.

(13) Trantzschel, T.; Bernarding, J.; Plaumann, M.; Lego, D.; Gutmann, T.; Ratajczyk, T.; Dillenberger, S.; Buntkowsky, G.; Bargon, J.; Bommerich, U. Parahydrogen Induced Polarization in Face of Keto-Enol Tautomerism: Proof of Concept with Hyperpolarized Ethanol. *Phys. Chem. Chem. Phys.* **2012**, *14*, 5601−5604.

(14) Kovtunov, K. V.; Truong, M. L.; Barskiy, D. A.; Salnikov, O. G.; Bukhtiyarov, V. I.; Coffey, A. M.; Waddell, K. W.; Koptyug, I. V.; Chekmenev, E. Y. Propane-d_6 Heterogeneously Hyperpolarized by Parahydrogen. *J. Phys. Chem. C* **2014**, *118*, 28234−28243.

(15) Koptyug, I. V.; Zhivonitko, V. V.; Kovtunov, K. V. New Perspectives for Parahydrogen-Induced Polarization in Liquid Phase Heterogeneous Hydrogenation: An Aqueous Phase and ALTADENA Study. *ChemPhysChem* **2010**, *11*, 3086−3088.

(16) Ratajczyk, T.; Gutmann, T.; Dillenberger, S.; Abdulhussaein, S.; Frydel, J.; Breitzke, H.; Bommerich, U.; Trantzschel, T.; Bernarding, J.; Magusin, P. C. M. M.; et al. Time Domain Para Hydrogen Induced Polarization. *Solid State Nucl. Magn. Reson.* **2012**, *43*−*44*, 14−21.

(17) Henning, H.; Dyballa, M.; Scheibe, M.; Klemm, E.; Hunger, M. In Situ CF MAS NMR Study of the Pairwise Incorporation of Parahydrogen into Olefins on Rhodium-containing Zeolites. *Chem. Phys. Lett.* **2013**, *555*, 258−262.

(18) Arzumanov, S. S.; Stepanov, A. G. Parahydrogen-Induced Polarization Detected with Continuous Flow Magic Angle Spinning NMR. *J. Phys. Chem. C* **2013**, *117*, 2888−2892.

(19) Obenaus, U.; Althoff-Ospelt, G.; Lang, S.; Himmelmann, R.; Hunger, M. *ChemPhysChem* **2017**, *18*, 455−458.

(20) Carson, P. J.; Bowers, C. R.; Weitekamp, D. P. The PASADENA Effect at a Solid Surface: High-Sensitivity Nuclear Magnetic Resonance of Hydrogen Chemisrption. *J. Am. Chem. Soc.* **2001**, *123*, 11821−11822.

(21) Koptyug, I. V.; Kovtunov, K. V.; Burt, S. R.; Anwar, M. S.; Hilty, C.; Han, S.; Pines, A.; Sagdeev, R. Z. Para-Hydrogen-Induced Polarization in Heterogeneous Hydrogenation Reactions. *J. Am. Chem. Soc.* **2007**, *129*, 5580−5586.

(22) Gutmann, T.; Ratajczyk, T.; Xu, Y.; Breitzke, H.; Grunberg, A.; Dillenberger, S.; Bommerich, U.; Trantzschel, T.; Bernarding, J.; Buntkowsky, G. Understanding the Leaching Properties of Heterogenized Catalysts: A Combined Solid-State and PHIP NMR Study. *Solid State Nucl. Magn. Reson.* **2010**, *38*, 90−96.

(23) Zhivonitko, V. V.; Kovtunov, K. V.; Beck, I. E.; Ayupov, A. B.; Bukhtiyarov, V. I.; Koptyug, I. V. Role of Different Active Sites in Heterogeneous Alkene Hydrogenation on Platinum Catalysts Revealed by Means of Parahydrogen-Induced Polarization. *J. Phys. Chem. C* **2011**, *115*, 13386−13391.

(24) Kovtunov, K. V.; Beck, I. E.; Bukhtiyarov, V. I.; Koptyug, I. V. Observation of Parahydrogen-Induced Polarization in Heterogeneous Hydrogenation on Supported Metal Catalysts. *Angew. Chem., Int. Ed.* **2008**, *47*, 1492−1495.

(25) Kovtunov, K. V.; Zhivonitko, V. V.; Corma, A.; Koptyug, I. V. Parahydrogen-Induced Polarization in Heterogeneous Hydrogenations Catalyzed by an Immobilized Au(III) Complex. *J. Phys. Chem. Lett.* **2010**, *1*, 1705−1708.

(26) Kovtunov, K. V.; Barskiy, D. A.; Salnikov, O. G.; Khudorozhkov, A. K.; Bukhtiyarov, V. I.; Prosvirin, I. P.; Koptyug, I. V. Parahydrogen-Induced Polarization (PHIP) in Heterogeneous Hydrogenation Over Bulk Metals and Metal Oxides. *Chem. Commun.* **2014**, *50*, 875−878.

(27) Salnikov, O. G.; Burueva, D. B.; Gerasimov, E. Y.; Bukhityarov, A. V.; Khudorozhkov, A. K.; Prosvirin, I. P.; Kovtunova, L. M.; Barskiy, D. A.; Bukhtiyarov, V. I.; Kovtunov, K. V.; et al. The Effect of Oxidative and Reductive Treatments of Titania-Supported Metal Catalysts on the Pairwise Hydrogen Addition to Unsaturated Hydrocarbons. *Catal. Today* **2017**, *283*, 82−88.

(28) Bouchard, L.-S.; Burt, S. R.; Anwar, M. S.; Kovtunov, K. V.; Koptyug, I. V.; Pines, A. NMR Imaging of Catalytic Hydrogenation in Microreactors with the Use of Para-Hydrogen. *Science* **2008**, *319*, 442−445.

(29) Kovtunov, K. V.; Beck, I. E.; Zhivonitko, V. V.; Barskiy, D. A.; Bukhtiyarov, V. I.; Koptyug, I. V. Heterogeneous Addition of H_2 to Double and Triple Bonds Over Supported Pd Catalysts: A Parahydrogen-Induced Polarization Technique Study. *Phys. Chem. Chem. Phys.* **2012**, *14*, 11008−11014.

(30) Henning, H.; Dornbach, M.; Scheibe, M.; Klemm, E.; Hunger, M. In Situ MAS NMR Investigation of the Hydrogenation of Acrylonitrile on Pt- and Rh-Containing Zeolites Y. *Microporous Mesoporous Mater.* **2012**, *164*, 104−110.

(31) Zhao, D.; Feng, J.; Huo, Q.; Melosh, N.; Fredrickson, G. H.; Chmelka, B. F.; Stucky, G. D. Triblock Copolymer Syntheses of Mesoporous Silica with Periodic 50 to 3000 Angstrom Pores. *Science* **1998**, *279*, 548−552.

(32) Obenaus, U.; Dyballa, M.; Lang, S.; Scheibe, M.; Hunger, M. Generation and Properties of Brønsted Acid Sites in Bifunctional Rh-, Ir-, Pd-, and Pt-Containing Zeolites Y Investigated by Solid-State NMR Spectroscopy. *J. Phys. Chem. C* **2015**, *119*, 15254−15262.

(33) Hunger, M.; Horvath, T. A New MAS NMR Probe for In Situ Investigations of Hydrocarbon Conversion on Solid Catalysts under Continuous-Flow Conditions. *J. Chem. Soc., Chem. Commun.* **1995**, 1423−1424.

(34) Buchholz, A.; Wang, W.; Arnold, A.; Xu, M.; Hunger, M. Succesive Steps of Hydration and Dehydration of Silicoaluminophosphates H-SAPO-34 and H-SAPO-37 Investigated by In Situ CF MAS NMR Spectroscopy. *Microporous Mesoporous Mater.* **2003**, *57*, 157−168.

(35) Hunger, M. In Situ Flow MAS NMR Spectroscopy: State of the Art and Applications in Heterogeneous Catalysis. *Prog. Nucl. Magn. Reson. Spectrosc.* **2008**, *53*, 105−127.

DOI: 10.1021/acs.jpcc.7b01899
J. Phys. Chem. C 2017, 121, 9953−9962

(36) Rabl, S.; Santi, D.; Haas, A.; Ferrari, M.; Calemma, V.; Bellussi, G.; Weitkamp, J. Catalytic Ring Opening of Decalin on Ir- and Pt-Containing Zeolite Y − Influence of the Charge-Compensating Alkali Cations. *Microporous Mesoporous Mater.* **2011**, *146*, 190−200.
(37) Matsui, T.; Harada, M.; Bando, K. K.; Toba, M.; Yoshimura, Y. EXAFS Study on the Sulfidation Behavior of Pd, Pt and Pd-Pt Catalysts Supported on Amorphous Silica and High-Silica USY Zeolite. *Appl. Catal., A* **2005**, *290*, 73−80.
(38) McVicker, G. B.; Baker, R. T. K.; Garten, R. L.; Kugler, E. L. Chemisorption Properties of Iridium on Alumina Catalysts. *J. Catal.* **1980**, *65*, 207−220.
(39) Kip, B. J.; Duivenvoorden, F. B. M.; Koningsberger, D. C.; Prins, R. Determination of Metal Particle Size of Highly Dispersed Rhodium, Iridium, and Platinum Catalysts by Hydrogen Chemisorption and EXAFS. *J. Catal.* **1987**, *105*, 26−38.
(40) Brunauer, S.; Emmett, P. H.; Teller, E. Adsorption of Gases in Multimolecular Layers. *J. Am. Chem. Soc.* **1938**, *60* (2), 309−319.
(41) Thielemann, J. P.; Girgsdies, F.; Schlogl, R.; Hess, C. Pore Structure and Surface Area of Silica SBA-15: Influence of Washing and Scale-Up. *Beilstein J. Nanotechnol.* **2011**, *2*, 110−118.
(42) http://www.zeolyst.com/our-products/standard-zeolite-powders/zeolite-y.aspx.
(43) Suzuki, I.; Oki, S.; Namba, S. Determination of External Surface Areas of Zeolites. *J. Catal.* **1986**, *100*, 219−227.
(44) Meier, W. M.; Olson, D. H.; Baerlocher, C. Atlas of Zeolite Structure Types. *Zeolites* **1996**, *17*, 1−230.
(45) Obenaus, U.; Neher, F.; Scheibe, M.; Dyballa, M.; Lang, S.; Hunger, M. Relationships between the Hydrogenation and Dehydrogenation Properties of Rh-, Ir-, Pd-, and Pt-Containing Zeolites Y Studied by In Situ MAS NMR Spectroscopy and Conventional Heterogeneous Catalysis. *J. Phys. Chem. C* **2016**, *120*, 2284−2291.
(46) Hesse, M.; Meier, H.; Zeeh, B. *Spektroskopische Methoden in der organischen Chemie*, ed. 8; Georg Thieme Verlag KG: Stuttgart, Germany, 2012; pp 229−247.

DOI: 10.1021/acs.jpcc.7b01899
J. Phys. Chem. C 2017, 121, 9953−9962